

Topical Perspectives

hCES1 and hCES2 mediated activation of epalrestat-antioxidant mutual prodrugs: Unwinding the hydrolytic mechanism using *in silico* approaches



Shalki Choudhary, Om Silakari*

Molecular Modeling Lab (MML), Department of Pharmaceutical Sciences and Drug Research, Panjab University, Patiala, Punjab, 147002, India

ARTICLE INFO

Article history:

Received 27 April 2019

Received in revised form

18 June 2019

Accepted 18 June 2019

Available online 20 June 2019

Keywords:

Epalrestat

Homology modeling

Human carboxylesterases

Pharmacophore analysis

Molecular dynamics

Molecular docking

ABSTRACT

Herein, we report four series of mutual prodrugs of epalrestat by combining it with different antioxidants using glycine, beta-alanine, and phenylalanine as a linker and by directly linking them through an ester linkage. The designed prodrugs were subjected to pharmacophore and docking-based virtual screening to determine the susceptibility of these prodrugs to be hydrolyzed by human carboxylesterases (hCES1 and hCES2). Five best prodrugs from each series were further submitted to detailed mechanistic study of hCES1 and hCES2 based hydrolytic activation using quantum mechanics and molecular dynamics approach. Additionally, Verloop's sterimol parameters (B1-B5, L) were calculated in order to investigate the steric constraint of prodrugs to the catalytic sites of hCES1 and hCES2 enzymes. Our results indicated that, among these prodrugs, EP-D4, EP-E13, EP-F5, and EP-F14 are best substrates for hCES1 while EP-G3 and EP-G15 are potential substrates for hCES2. On the other hand, EP-D19 serves as good substrates for both enzymes.

© 2019 Elsevier Inc. All rights reserved.

1. Introduction

Epalrestat is an acetic acid derivative and only aldose reductase (ALR2) inhibitor available in the market of Japan, India, and China for the management of diabetes-associated complications such as neuropathy, nephropathy, and retinopathy [1–3]. Under hyperglycaemic conditions, epalrestat reduces accumulation of intracellular sorbitol, implicated in the pathogenesis of diabetic complications (DC) [4].

At the molecular level, mainly four hypotheses, such as polyol pathway flux (upstream pathway), protein kinase C (PKC), hexosamine pathway flux, advanced glycation end products (AGEs) formation, have been proposed to be implicated in the pathogenesis of DC [5]. A most popular hypothesis is the polyol pathway (upstream pathway), in which ALR2 and sorbitol dehydrogenase (SDH) are two rate-limiting enzymes. Prolonged hyperglycemia induced overproduction of superoxide by mitochondrial electron-transport chain also increases oxidative stress (downstream pathway) that activates the nuclear enzyme, poly (ADP-ribose) polymerase-1 (PARP) which further decreases the activity of glyceraldehyde-3-

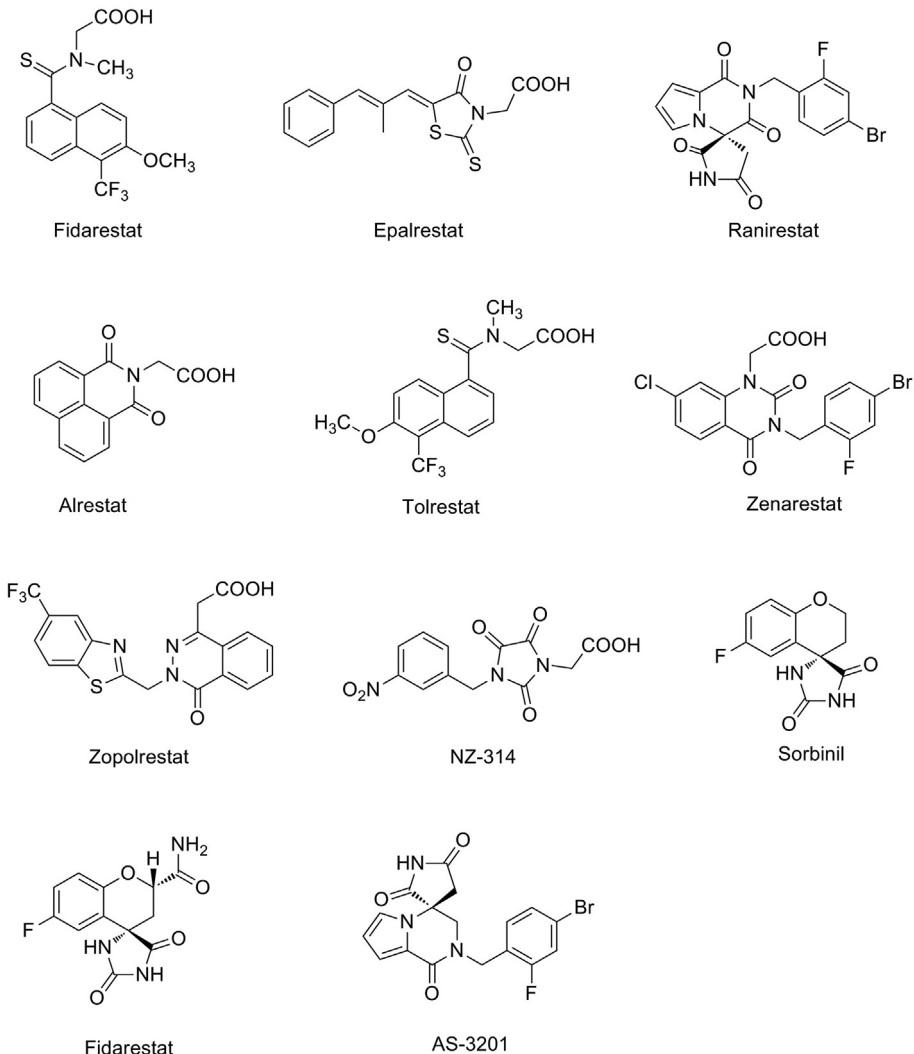
phosphate dehydrogenase (GAPDH) and triggers all the four pathways of DC [6]. Due to highly complex pathology of diabetic complications, single target drug therapy is not as effective as it requires for the management of these conditions, as the disease can progress through another pathway even after blocking the one pathway. Moreover, the partial inhibition of multiple targets is more effective than complete inhibition of a single target. Benfotiamine is one such example of multi-targeted agent effective in the treatment of diabetic retinopathy, neuropathy and nephropathy which acts by blocking three major biochemical pathways, namely, hexosamine pathway, advanced glycation end products (AGEs) formation pathway and diacylglycerol (DAG)-protein kinase C (PKC) pathway, but is still in clinical trials and seeking FDA approval.

Drugs currently in clinical trials or used as a therapy for the treatment of DC are mostly ALR2 inhibitors. Some of the well-known ALR2 inhibitors are displayed in Fig. 1.

For now, as such, there is no effective drug available in the market against DC, except ALR2 inhibitor epalrestat, which is official in Japanese pharmacopeia but did not get FDA approval due to limited clinical applicability and some significant side effects [7,8]. Moreover, epalrestat is single targeting agent and only capable of blocking the upstream pathway (polyol pathway) of DC; therefore, there are chances for the disease to progress through other

* Corresponding author.

E-mail address: omsilakari@gmail.com (O. Silakari).

**Fig. 1.** Some well-known ALR2 inhibitors.

pathways even after blocking the one pathway. Apart from this, one more limitation is that the epalrestat is currently being prescribed as an immediate release drug, thus administered three times a day (50 mg 3 times/day) and have short elimination half-life (1 h) [9]. In order to provide an effective one-day treatment therapy with minimum side effects, and to improve the elimination half-life of epalrestat, there is need of modified release approach (sustained release, controlled release or delayed release). The modified release of epalrestat can be achieved by designing sustained, controlled and delayed release formulation. In one of the embodiments of a patent, it is claimed that the modified release of epalrestat can also be achieved by prodrug designing, by covalently linking epalrestat through ester and amide linkage [10]. In light of the above, designing of ester and amide-linked prodrugs of epalrestat with multi-targeting ability can be an interesting approach for the effective management of diabetic complications. It has been reported that the antioxidants are also fruitful in the management of DC by free radical scavenging and gastro-protective effect and act on all the four molecular pathways [11–13]. Thus, some epalrestat based mutual prodrugs were designed by derivatizing free -COOH group into amides and esters using an amino group of antioxidant-loaded linkers and the hydroxyl group of antioxidants themselves respectively. These prodrugs are expected to target both upstream

and downstream pathways of DC, improve therapeutic index owing to a synergistic effect, may provide sustained release and improve the elimination half-life of parent drug (epalrestat).

Since the ester and amide prodrugs are biotransformed through hydrolytic cleavage by carboxylesterase (CES) enzymes, understanding the mechanism of this enzyme catalyzed hydrolytic cleavage may provide effective designing of these prodrugs. *In-silico* techniques like molecular docking, quantum mechanics (QM)/molecular mechanics (MM) and molecular dynamics (MD) can be used to explore various reactions involved in hydrolysis or biotransformation of different drugs at the molecular level [14,15]. Combination of QM/MM and MD calculations takes into consideration the structural and dynamic features of both protein and substrate. These approaches help in investigating the key active site residues involved in the biotransformation of ester-containing drugs, thus, unwind their molecular mechanism [14]. The same approaches can be utilized to disclose the CES mediated hydrolytic mechanism of mutual prodrugs with ester and amide linkage, designed against diabetic complications.

A plethora of knowledge has been accumulated about the CES enzymes which belong to carboxylesterase (CES) superfamily and majorly divided into CES1, CES2, CES3 and CES4 [15–17]. Enzymes hCE1 and hCE2 which belongs to family CES1 and CES2 respectively

are most frequently involved enzymes for metabolic activation of amide and ester prodrugs [18]. As per their classification, CES1 family covers human liver carboxylesterase (HU1) and human brain carboxylesterases (hBr1, hBr2, and hBr3) while CES2 family involves human livercarboxylesterase (HU3) and human intestine-carboxylesterase (HSICE) [18].

The hydrolysis of ester and amide prodrugs is an example of nucleophilic substitution (NS). For this NS reaction to be carried out efficiently by CES enzymes, substrate molecule and enzyme substrate molecule should satisfy certain stereoelectronic requirements. On the basis of literature reports, as far as geometrical aspects are a concern, both hCES1 and hCES2 have different geometries and catalyze different types of substrates. Due to the small catalytic domain, hCES1 can catalyze the prodrugs with small aryl/alkyl unit. On the contrary, hCES2 has a large catalytic domain and cleave the prodrugs with large alkyl/aryl unit. This fact can be better explained by calculating sterimol steric parameters i.e. B1-B5 and L which were introduced by Verloop in 1976 [19].

The catalytic triad of both hCES1 (Ser221, Glu354, His468) and hCES2 (Ser228, Glu345, His457) play an important role in carboxylesterases mediated hydrolysis. In both triads, Ser221 and Ser228 act as a nucleophile in the catalytic hydrolysis of mutual prodrugs (carbonyl carbon of amide and ester as an electrophile). Thus, the HOMO (which characterize nucleophilicity of -OH of serine) and LUMO (which characterize electrophilicity of carbonyl carbon of ester) energy gap can be calculated to determine the susceptibility of hydrolysis of esters. Fukui was the first to suggest the utility of the HOMO and LUMO in chemical reactions. It has been reported that a small energy gap indicates high chemical reactivity, thus an important factor for the determination of the feasibility of a chemical reaction [20,21]. Considering this fact, the HOMO energy of nucleophiles (serine), LUMO energy of electrophile (mutual prodrugs) and HOMO-LUMO energy gap were calculated to justify the predicted catalytic hydrolytic activity of designed prodrugs. Geometrical parameters like Burgi-Dunitz angle and distance were also found to be effective in nucleophilic substitution involved in this type of hydrolytic cleavage. The quantum mechanical approach was applied to determine the HOMO-LUMO energy gap and geometrical parameters (Burgi-Dunitz angle and distance).

In short, this study is simply an *in-silico* guided approach for rationally designing some epalrestat-antioxidants mutual prodrugs by applying molecular mechanics, quantum mechanics and molecular dynamics approaches. Additionally, it is a comparative study of hCES1 and hCES2 mediated hydrolysis of ester and amide-linked epalrestat-antioxidant mutual prodrugs, which in future can be optimized for the management of DC.

2. Material and methods

2.1. Pharmacophore generation

For the development of ligand-based pharmacophore model, a dataset of 31 hCES1 substrates and 37 hCES2 substrates were selected on the basis of their reported Km values [22,23]. Further, the pKm values were calculated by taking -log of Km values and used for pharmacophore generation. The pharmacophore models were developed for hCES1 and hCES2 using the PHASE module of Schrödinger. The idea behind generating a pharmacophore model is to identify the common and essential features along with intra-feature distances present in the mutual prodrugs which are to be hydrolyzed by the hCES1 and hCES2. These generated models can be further used for the prediction of the hydrolytic activity of the enzymes. Initially, the dataset molecules were divided into active, moderately active and inactive categories on the basis of pKm values describing the hydrolytic activity of hCES1 and hCES2.

Afterward, these molecules were subjected to conformer generation by employing Monte Carlo Minimization Method (MCMM)/ Low Mode Docking (LMD) algorithm within an energy threshold of 20 kcal/mol. The generated conformers were utilized to search for the common pharmacophoric features and variants by considering six pharmacophoric features i.e. hydrogen bond acceptor, hydrogen bond donor, hydrophobic, ring aromatic, positive ionizable and negative ionizable [24,25]. The sampled conformational space of each molecule was applied for developing the model. Various pharmacophore hypotheses were generated that were later ranked on the basis of scoring parameters i.e. survival (S) and survival minus inactive (S-I) score [26]. Following the hypotheses generation and ranking, the generated hypotheses were clustered and then selected the representative hypotheses of each cluster based on the highest S-I score. The selected hypotheses were used to align the molecules that were not considered for the pharmacophore generation (non-modeled molecules). Finally, 3D-QSAR was built for the prediction of hydrolytic activity [27].

2.2. Homology modeling

Since the 3-D structure of hCES2 is not available in a protein data bank (PDB), the homology model of this enzyme was developed using 1MX1 as a template protein by Modeller 9.16 [28]. The 559 amino acid sequence of hCES2 (cocaine esterase) was obtained from UniProt (ID:O00748) and then template protein was identified in NCBI site using Basic Local Alignment Search Tool (BLAST) run [29]. The identified template protein (hCES1, PDB ID: 1MX1) was then used for building a homology model of the target protein. Total five models were generated which were validated using protein quality (ProQ), protein structure-activity (ProSA) [30,31] and qualitative model energy analysis (Qmean) tools to gauge the quality of modeled proteins [32]. The modeled protein was further validated by the Ramachandran plot obtained from RAMPAGE program. Among all the generated models, the best model was selected with least root mean square deviation (RMSD) value by superimposing it over template protein and on the basis of MolPdf and discrete optimized protein energy (DOPE) scores [33].

2.3. Molecular docking, prime MM-GBSA, ADME, and molecular dynamics

Docking study was performed to find out the putative binding pose of the prodrugs within the active site of the proteins. For molecular docking study, number of Epalrestat based mutual prodrugs were sketched by considering various antioxidants including 7 flavones, 2 coumarins, 6 terpenes, 6 benzoquinones (BQ) linked phenols, 1 naphthoquinone (lawsone), 1 cinnamic acid derivative (Methylferulic acid) and 1 anisole derivative (Butylatedhydroxyanisole (BHA)) as a promoiety. Total 24 different antioxidants were used for the designing of mutual prodrugs on the basis of synthetic possibility. All the sketched prodrugs were cleaned by utilizing the "builder tool" option in "Maestro" 9.2 molecular modeling environment. The molecules were optimized with OPLS_2005 force-field using the "Ligprep" module of Maestro at a pH range of 7 ± 0.5 [34].

The crystal structure 1YA8 of hCES1 was used for docking analysis to study its hydrolytic action. This structure was selected on the basis of resolution and previously reported information including catalytic water, amino acid triad and optimum distance of catalytic water to amino acid triad involved in hydrolysis [35]. Moreover, the co-crystallized ligand of 1YA8 is mevastatin which is ester containing substrate and mimic the hydrolytic mechanism with designed prodrugs. The crystal structure of the above-mentioned protein was availed from public domain i.e. PDB (www.rcsb.org)

and prepared in “Protein Preparation Wizard”. Since the crystal structure of hCES2 was not available on PDB, the homology model for hCES2 was developed by considering 1MX1 as a template protein.

Further, the binding free energies (kcal/mol) of the prodrug-protein complex were calculated using prime MM/GBSA module of “Maestro” 9.2 based on the equation:

$$\text{MMGBSA } \Delta G_{\text{bind}} = \text{ER: EL} - \text{EL} - \text{ER}$$

Where ER: EL, EL, and ER are the prime energies of the optimized complex, free ligand, and free receptor, respectively [36].

The ADME properties of all synthesized compounds were also calculated using QikProp module available in Schrödinger. The stability of the highest active prodrugs was accessed by molecular dynamics simulations (MDS) for the period of 30ns, using a freely available academic version of “Desmond” program. The solvent system was built around the protein-ligand complex using the TIP3P water model and the shape of the box was kept as orthorhombic with dimensions $10 \times 10 \times 10 \text{ \AA}$ [37]. The neutralization of physiological pH of the system was done by adding the Na^+ counterions and the salt concentration was set as 0.15 M. After the energy minimization, the constant temperature was maintained with Nose-Hoover chain thermostat to attain NPT equilibration at 310K, while, constant pressure was acquired using the MartynTobias-Klein barostat. The MDS was performed under the periodic boundary conditions in order to avoid edge effects. The simulations were performed at a time step of 1 fs and 10 ps as recording time. Thereafter, RMSD was calculated using the desmond protocol i.e. simulation interaction diagram for the protein-prodrug complex [38]. Subsequently, geometrical parameters like Burgi-Dunitz angle and distance were also calculated.

2.4. Quantum mechanical calculations

The various quantum mechanical parameters were calculated using Schrödinger (9.3), where the molecular structures were optimized geometrically by employing a semi-empirical method at Recife Model 1 (RM1) [39,40]. Frontier molecular orbital approach was utilized to calculate the energy of the highest/lowest occupied/unoccupied molecular orbitals (HOMO/LUMO) and the energy gap ($\Delta E = E_{\text{LUMO}} - E_{\text{HOMO}}$) [41]. Subsequently, various global reactivity parameters like chemical hardness (η), chemical potentials (μ) and the electrophilicity index (ω) were computed using the following formulas [42].

$$\mu = -\chi = \frac{-I + A}{2}$$

$$\eta = I - A$$

$$\omega = \frac{\mu^2}{2\eta}$$

Where χ is electronegativity of the system.

2.5. Verloop'ssterimol calculation

The Verloop'ssterimol parameters i.e. SMB1-5 and L1 were calculated using the “sterimol” module of the molecular operating environment (MOE), where SMB1 and SMB5 represent the minimum and a maximum width of the substituent. These parameters are representative of the size and shape of the substituents [43].

3. Results and discussion

3.1. Putative Epalrestat based mutual prodrugs

In this study, a total of 87 Epalrestat-antioxidants mutual prodrugs were designed on the basis of synthetic possibilities and these prodrugs were then subjected to *in-silico* prediction of hCES1 and hCES2 mediated hydrolysis. Structural details of the designed mutual prodrugs are summarized in Table 1.

3.2. Pharmacophore generation and 3D QSAR analysis

In the present study, a diverse dataset of 31 substrates of hCES1 and 37 substrates of hCES2, collected from the various literature reports [22,23], were utilized for the development of two separate pharmacophore models of these enzymes which are responsible for the hydrolysis of ester and amide containing mutual prodrugs. For this purpose, the substrates were divided into active, inactive and moderately active molecules according to their pK_m values. In the case of hCES1 substrates, the activity threshold value was kept in a range of 3.5–5 μM . For this, total of 10 molecules were considered active, 8 were considered inactive and remaining were placed in a moderately active group. On the other hand, for hCES2, the activity threshold was kept in the range of 3.401–5 μM and molecules were divided as 14 active, 10 inactive and 13 moderately active. The conformational space of all substrates was explored using mixed MCMM/LMDO macro models. Maximum 250 conformations were generated for each substrate within an energy window of 20 kcal/mol and 1 \AA RMSD to avoid unnecessary conformers. To find common pharmacophore features, minimum 4 and maximum 5 sites were selected and models were restricted to match at least 10 and 14 common hypotheses for hCES1 & 2 respectively. This number was selected on the basis of active molecules considered for both enzymes so that it could align with all the active molecules. Total 133 hypotheses were generated for hCES1 and 22 hypotheses were generated for hCES2. The overall ranking of all generated hypotheses was done according to their survival and survival minus inactive (S-I) scores. A higher value of S-I represents the hypothesis

Table 1

Structural details of designed mutual prodrugs.

Mutual prodrugs	Total mutual prodrugs	Linkage	Total mutual prodrugs
Target-hCES1 & 2	24 EP(D1-D24)	without linker	15 EP(G1-G15)
With linker	24 EP(E1-E24)	Ester linkage	
Epalrestat-[COOH + NH ₂]-Linker-[COOH + OH]-Antioxidants	24 EP(F1-F24)	Epalrestat-[COOH + OH]-Antioxidants	
Linker used			
Glycine			
β -Alanine			
Phenylalanine			

which is more likely to pick the active molecules. Further, to avoid the same hypotheses, all generated hypotheses were clustered. From all resulting clusters, the one with highest S-I score from each cluster was selected to give top-ranked candidate hypothesis for both hCES1 & 2. Among these top-ranked hypotheses, the best one was selected on the basis of the S-I score for further analysis. The hypothesis scores of best hypotheses for hCES1 & 2 are displayed in **Table 2**.

Further, 3D-QSAR models for both hCES1 & 2 were developed to establish a correlation between dependent (hydrolytic activity) and independent (structural features) variables. The whole dataset was divided into training and test set by equally distributing actives, inactive and moderately actives in each set. The molecules in the

training set were aligned which was further used for the development of QSAR model. The best hypothesis for both hCES1 & 2 was selected on the basis of highest Q^2_{test} values with PLS 4 and 2 respectively. The statistical results of developed QSAR models for both enzymes are displayed in **Table 3**.

Generated model of hCES1 with hypothesis ID AAHRR.430 consists of five features including two hydrogen bond acceptor (A), one hydrophobic (H) and two ring aromatic (R). Similarly, the model of hCES2 with hypothesis ID AHHR.21 has four features i.e. one hydrogen bond acceptor (A), two hydrophobic (H) and one ring aromatic (R). Both models displayed a higher value of R^2_{train} , Q^2_{test} and Pearson-r corresponding to PLS 4 & 2. The high value of R^2 (correlation coefficient) and Q^2 (cross-validated correlation coefficient) indicates the close correlation between experimental and predicted activities of both test and training sets. Also, the higher value of Pearson-r justifies the good external predictive ability of both models. A correlation graph was plotted between experimental and predicted activities of test sets and training sets obtained from the best model of hCES1 & 2, as depicted by the scatter plot in **Fig. 2**.

The intrafeature distance between each feature of the best model was also calculated. Pharmacophore models of both enzymes were also mapped over their corresponding most active

Table 2
Hypothesis score of best hypothesis for hCES1 & 2.

Hypothesis ID	Survival score	S-I score	Site	Vector	Volume	Matches
For hCES1 AAHRR.430	45.991	44.851	0.82	0.911	0.708	9
For hCES2 AHHR.21	41.589	40.590	0.60	0.846	0.466	14

Table 3
Statistical results of the developed 3D-QSAR model for hCES1 & 2.

Model ID	PLS factor	SD	R^2_{train}	F value	Stability	RMSE	Q^2_{test}	Pearson-r
For hCES1 AAHRR.430	4	0.065	0.997	176	0.559	0.597	0.823	0.949
For hCES2 AHHR.21	2	0.288	0.944	161	0.357	0.621	0.633	0.796

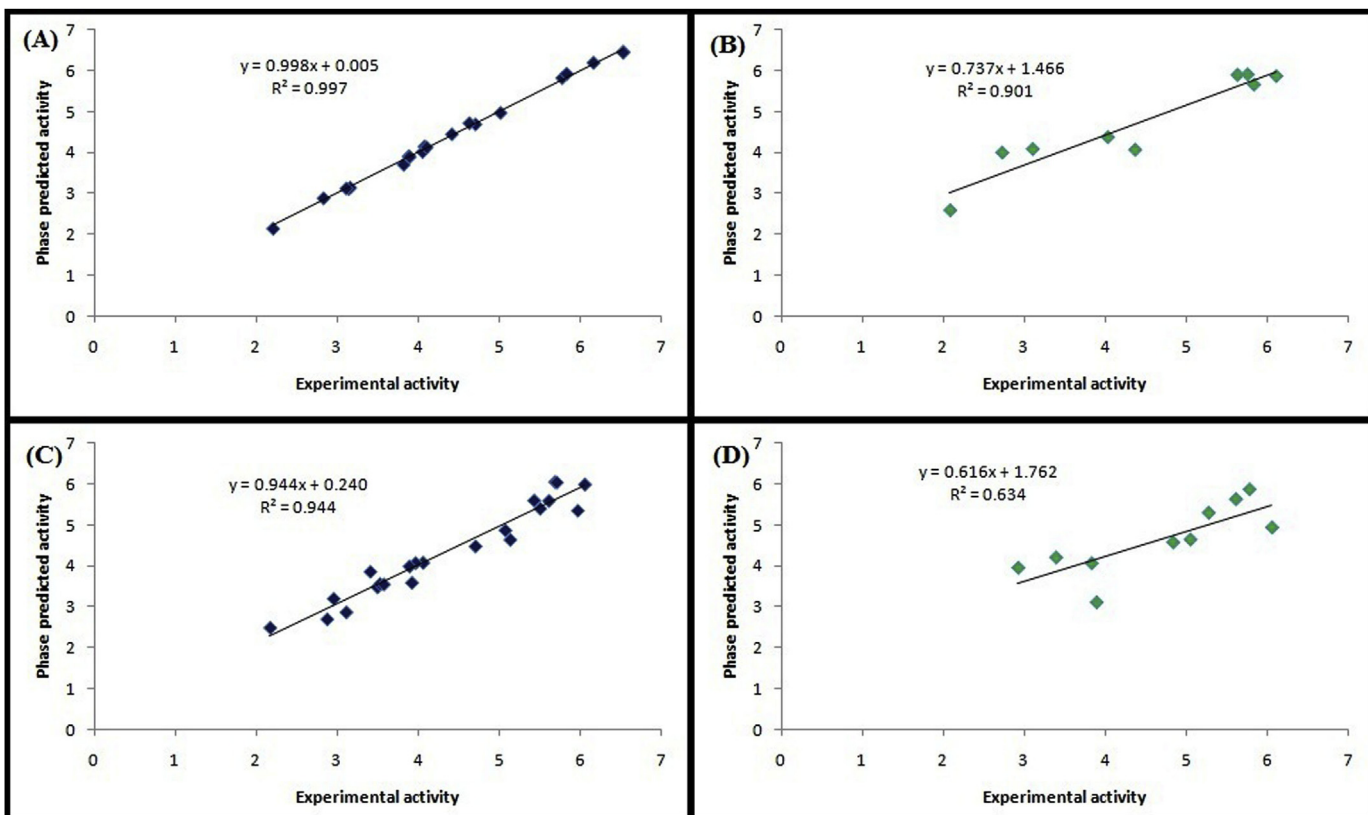


Fig. 2. Graphical representation of the correlation between experimental and predicted activities of training set substrates of hCES1 (A), the test set substrates of hCES1 (B), the training set substrates of hCES2 (C), and the test set substrates of hCES2 (D).

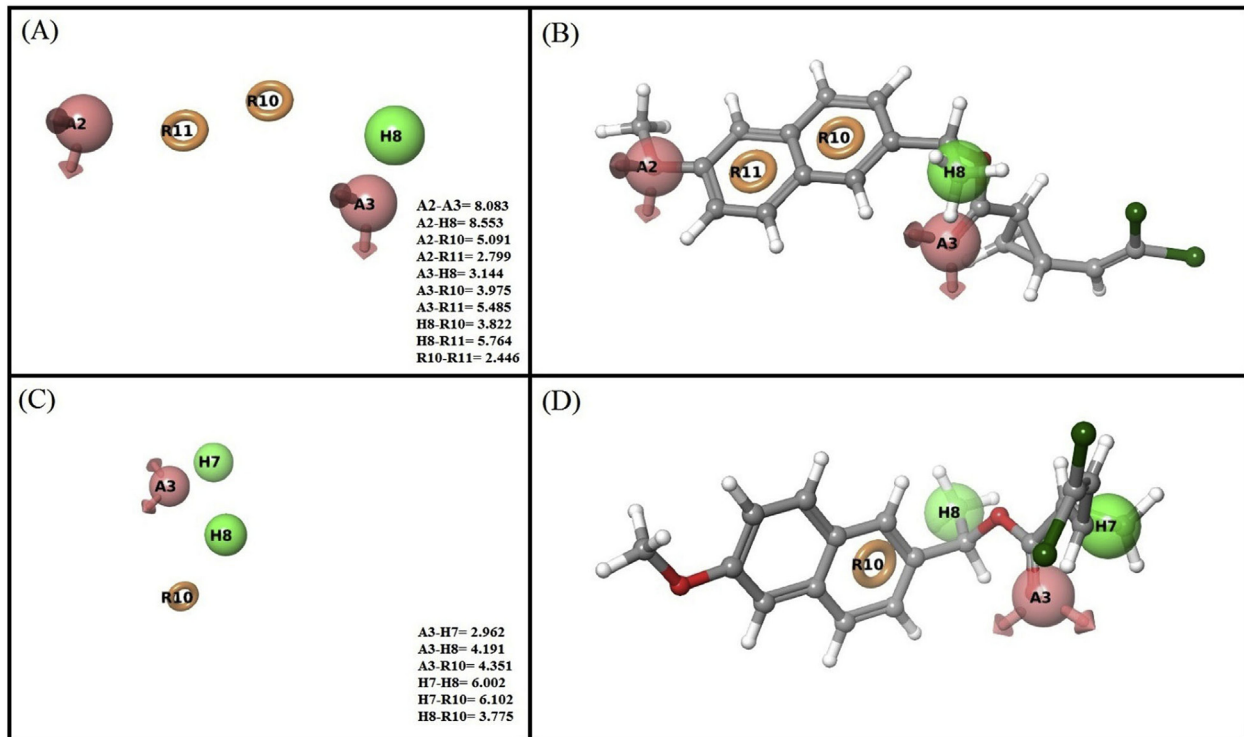


Fig. 3. The intrafeature distance of best pharmacophore model of hCES1 with hypothesis ID AAHRR.430 (A), mapped pose of AAHRR.430 over the most active molecule (B), Intrafeature distance of best pharmacophore model of hCES2 with hypothesis ID AHHR.21 (C), mapped pose of AHHR.21 over the most active molecule (D).

training molecules. Pictorial presentation of mapped models and calculated intrafeature distance are displayed in Fig. 3.

3.3. Validation of the pharmacophore model

Eventually, the developed pharmacophore models were validated using the test set of substrates to confirm the predictive ability. Both models were validated by four different methods and results

were found to be within the acceptable limit. In Y-randomization, the best models of hCES1 and 2 showed R^2_{scramble} values 0.908 and 0.823 respectively, which were lower than their corresponding original values of R^2_{train} , confirming the robustness of selected models. The calculated APD of test set molecules were also found to be within the threshold APD of training set molecules hence proves the reliability of developed models for their predictive ability for new molecules. Additionally, the values of Globraikh and Tropasha statistical

Table 4
Pharmacophore model validation parameters for hCES1 and hCES2.

validation method	validation parameters		
Y-randomization	PLS hCES1 4 hCES2 2	R^2_{scramble}	Q^2
		0.908	0.806
		0.823	0.624
Applicability domain (APD)	hCES1 Test set molecules 1A 1B 1C 1D 1E 1F 1G 1H 1I	Distance APD (4.865)	Test set molecules 2A 2B 2C 2D 2E 2F 2G 2H 2I 2J
		0	0
		3.316	3
		0	0
		4.795	0
		3.605	3.316
		3	4.582
		0	3
		0	3.605
		2.449	2.828
			2.236
Globraikh and Tropasha	hCES1 K K' R^2_0 R^2_0	0.948 1.039 0.949 0.983	hCES2 K K' R^2_0 R^2_0
			1.005 0.977 0.998 0.999
Screening based validation (Zinc Decoy database)	hCES1 Enrichment factor (EF) The goodness of hits (GH)	19.92 0.52	hCES2 Enrichment factor (EF) The goodness of hits (GH)
			17.57 0.53

parameters for both models fell under the acceptable limit, hence prove their prediction reliability. Both models were also validated using Zinc database of decoys and showed acceptable values of Enrichment factor (EF) and Goodness of hits (GH). All validation parameters related data is displayed in **Table 4**.

3.4. Prediction of hydrolytic activity

The best pharmacophore models of hCES1 & 2 were utilized to predict the hydrolytic activity of hCES1 & 2 enzymes for the biotransformation of putative Epalrestat based mutual prodrugs

designed on the basis of synthetic possibility. Total 87 mutual prodrugs were screened for hCES1 & 2 mediated hydrolysis. The retrieved hybrids were then subjected to molecular docking as well as molecular dynamics simulations. Predicted hydrolytic activity of all screened hybrids along with their glide score and MM-GBSA scores are given in **Table S1** (Supplementary data).

3.5. Homology modeling

The BLAST was run using FASTA format of protein to identify the template protein with maximum identity. On the basis of results

Fig. 4. Alignment of target protein over template protein.

obtained from BLAST run, 1MX1 protein (47% identity) was selected as a template protein. The targets sequence was then aligned over template protein and alignment file of the target-template protein was retrieved from public domain resource PROMALS3D (Fig. 4). Total 5 models were built and the 3D structures of target protein were obtained from modeler 9.19 software. Developed models were ranked on the basis of RMSD, MolPdf and DOPE scores. The model with lower RMSD, MolPdf and DOPE score is considered to have more similarity with template protein, thus model 1 was recognized as best model with MolPdf value and DOPE score 7127.40381 and -62373.4609 respectively. Modeled protein was then superimposed over template protein to find out their structural similarity in terms of RMSD value. Model 1 was found to have a minimum RMSD (0.960 Å). The superimposed pose of the template and the target protein is shown in Fig. 5. The quality of generated models was assessed using different tools such as ProQ, ProSA, and QMean. The scores obtained from different validation methods are summarized in Table 5. The global and local quality of all models was also evaluated in terms of Z-score and energy respectively (Fig. 6).

Additionally, the modeled protein was also validated by Ramachandran plot obtained from RAMPAGE program. Ramachandran plot of the target protein is shown in Fig. 7. Further, the stability of the homology model was assessed by running molecular dynamic simulations for a period of 100 ns (Fig. 8). On the basis of validation

parameters, we concluded that the modeled protein was of good quality and not build by chance.

3.6. Molecular docking, prime MMGBSA, and molecular dynamic simulations

The molecular docking makes a stable complex of protein and prodrugs which led to the identification of key features in hCES1 and 2 required for the hydrolysis of mutual prodrugs. The molecular docking analysis was performed for designed mutual prodrugs using the co-crystallized 3D structure of 1YA8 (hCES1) and developed homology model (hCES2) that displayed all the essential interactions which are required for the hydrolysis by both these proteins. Since Ser221 and Ser228 are key amino acids which play an important role in catalytic hydrolysis through hCES1 and 2 respectively, the interactions with these amino acids are crucial. Almost all prodrugs showed interactions with Ser221 (hCES1) and Ser228 (hCES2) with good glide score. After molecular docking studies, the mutual prodrugs were subjected to MMGBSA score calculation, to determine their affinity for hCES1 and hCES2 in terms of binding energy. Almost all prodrugs showed good affinity having binding energy in the range of -116 to -50 kcal/mol (Supplementary Table S1). Further, evaluating the pharmacokinetic parameters of all the prodrugs led to the identification of the prodrugs with optimum ADME properties. The values of all the parameters were found under acceptable limit as described in the Lipinski's rule of five (Supplementary Table S2) [44]. On the basis of results obtained from above-described analysis, the best five prodrugs from each series were selected and then subjected to molecular dynamics (MD) simulations for a period of 30ns in order to find out the stability of the docked prodrug-protein complex. The RMSD of the protein backbone was found to be within a range of 2.5–3.5 Å, signifying the stability of complex during the simulation period. The MD simulations disclosed that almost all prodrugs maintained the key interactions with catalytic amino acids for the whole simulation period. The simulation interaction diagram of mutual prodrug EP-D19, which is expected to get hydrolyzed by both the enzymes, with the active site of hCES1 and hCES2 along with the RMSD plots for backbone atoms are shown in Fig. 9. The predicted activity, MMGBSA and glide score of the best five prodrugs selected from each series are mentioned in Table 6.

Further, the hydrolytic efficiency of hCES1 and 2 was determined from some geometrical parameters such as Burgi-Dunitz angle (α_{BD}) and distance which ensure the favourability of nucleophilic attack over an electrophile. Here, Serine 221 and Serine 228 are the reported nucleophiles in case of hCES1 and 2 respectively, while the carbonyl groups of mutual prodrugs act as electrophilic centers. Thus, the distance and angle between these entities were calculated to compare the hydrolytic effect of this isoform of CES



Fig. 5. Superimposition of target protein homology model (hCES2) over template protein (PDB-1MX1).

Table 5
Validation score for all constructed models.

Model	Modeller	Modeller	RAMPAGE	ProQ	ProQ	ProSA	Qmean score	RMSD
	MolPdf	(Z-DOPE)	(%) ^a	LG SCORE	MaxSub	(Z-score)	(Z-score) ^b	(Å) ^c
1.	7127.40381	-62373.4609	94.1, 5, 0.9	4.645	0.334	-8.72	0.67, -2.66,	0.960
2.	7490.23828	-61835.7695	—	4.637	0.355	-8.72	—	0.964
3.	7371.63477	-62158.8046	—	4.520	0.343	-8.31	—	0.968
4.	7801.80713	-61911.8867	—	4.254	0.322	-8.56	—	0.962
5.	7288.70654	-62370.7851	—	4.580	0.337	-8.51	—	0.978

The lower value of DOPE score i.e. higher negative value represents the best model.

Lower the value of MolPdf best will be the quality of the generated model.

^a Values correspond to the % of residues that are located in the most favored, allowed and disallowed regions respectively.

^b The first value corresponds to the Qmean4 score, while the second value refers to the QMEAN Z-score.

^c RMSD value of target protein (hCES2 model) compared to the 3D structure of the template (1MX1) used for alignment.

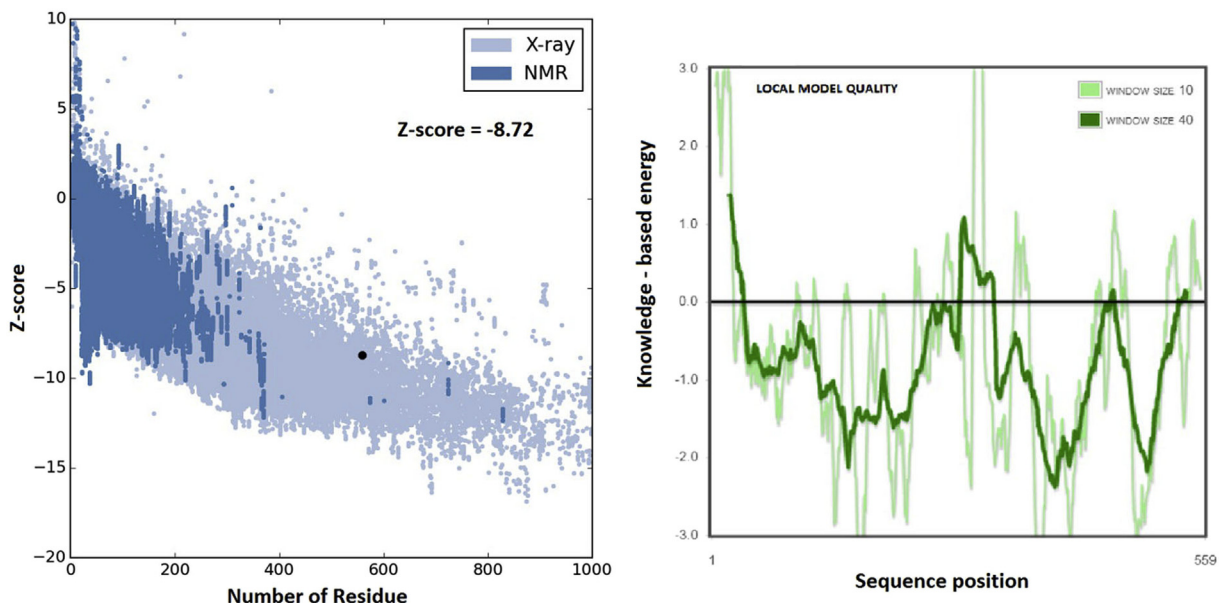


Fig. 6. Quality assessment of target protein (hCES2) using ProSA tool, global model quality in terms of Z-score score (left side) and local model quality in terms of energy as a function of amino acid sequence position (right side).

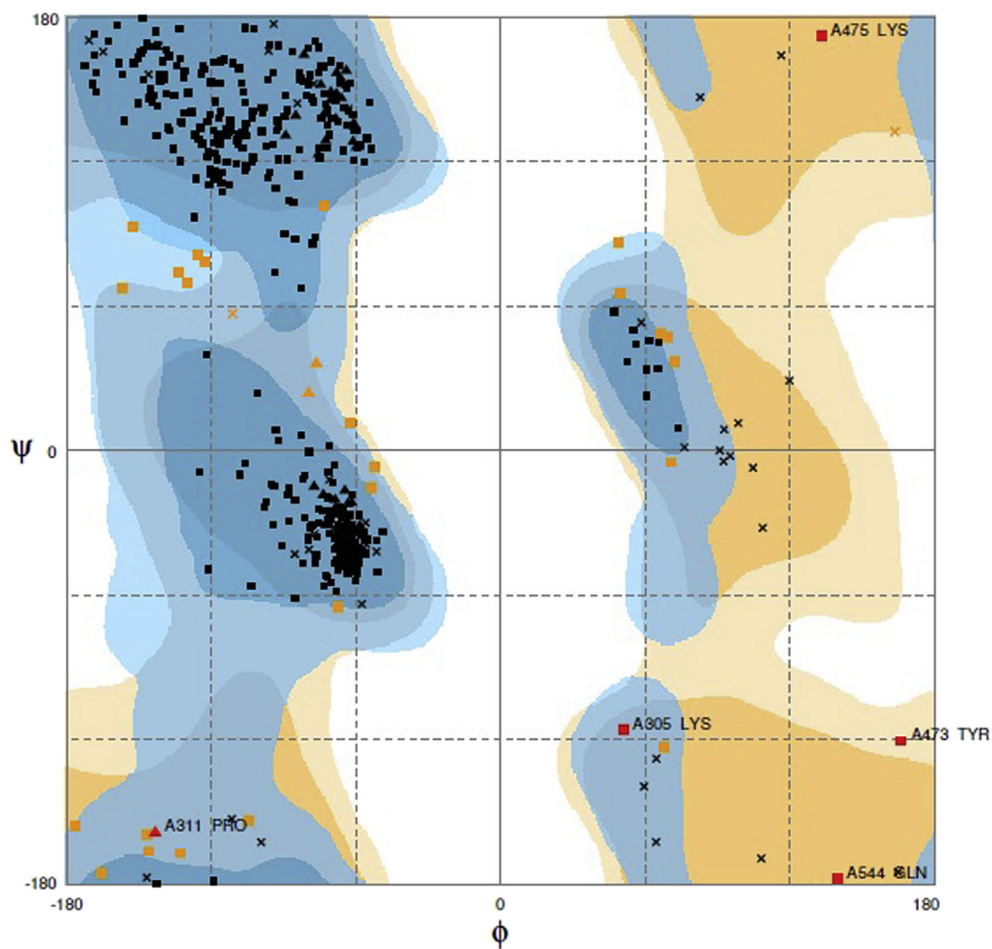


Fig. 7. Ramachandran plot of the target protein (hCES2) obtained from RAMPAGE.

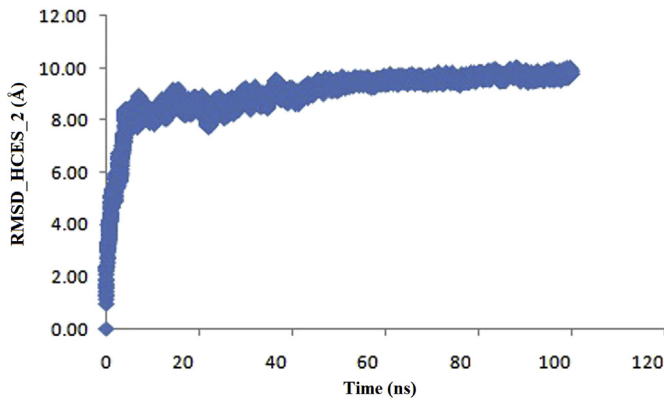


Fig. 8. RMSD plot of the target protein (hCES2) to ensure the stability of modeled protein throughout the period of 100 ns.

enzymes. Although, it is evident from the literature reports that, for the most favorable nucleophilic attack and efficient hydrolysis, there should be an obtuse angle (range $105 \pm 10^\circ$) between the plane of the nucleophile and an electrophile, however, some of our prodrugs could not fulfill the criteria of an obtuse angle. Our results

indicated that both the amide and ester carbonyl of mutual prodrug EP-D19 maintained the favorable angle and distance to get hydrolyzed by both hCES1 and hCES2 respectively. The Burgi-Dunitz angle and distance favorable for nucleophilic attack of Ser221 and Ser228 over ester and amide carbonyl of EP-D19 are shown in Fig. 10.

Prodrugs EP-E13, EP-F5, and EP-F14 manifested favorable angle and distance for the nucleophilic attack in case of hCES1. On the other hand, in the case of hCES2, prodrug EP-G15 has maintained the favorable angle required for hydrolysis but failed to maintain distance. On the contrary, EP-G7 has maintained the favorable distance but failed to acquire the favorable angle. The Burgi-Dunitz angle and distance for the mutual prodrugs have been displayed in Table 7.

Note: In case of 6-Aminoflavones i.e. EP-D4 and EP-F4 all values are for amide carbonyl and not for ester carbonyl, as these prodrugs contain two amide linkages but no ester linkage. On the other hand, in the case of ester linked (EP-G) category, all values are for the ester group.

3.7. Quantum mechanical calculations

Molecular orbital theory investigates the electronic flow from

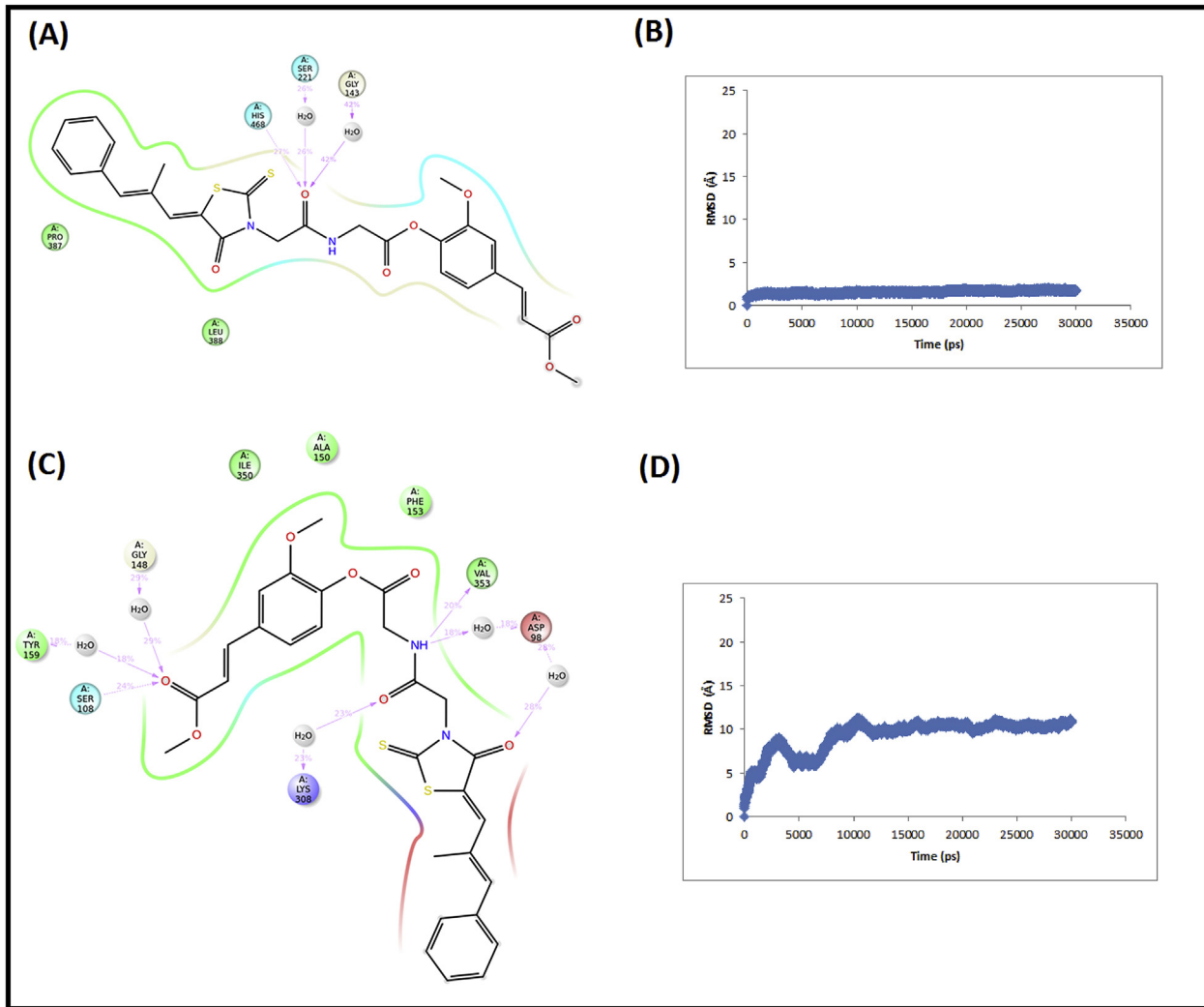


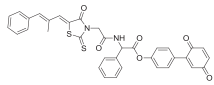
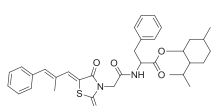
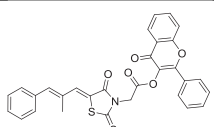
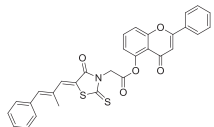
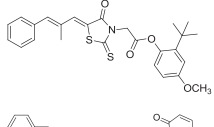
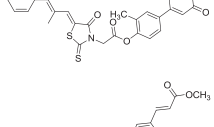
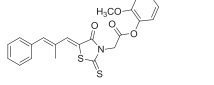
Fig. 9. Simulation interaction diagram of EP-D19 complexed with the active site of hCES1 (A) along with the RMSD plot of backbone atoms (B) and simulation interaction diagram of EP-D19 complexed with the active site of hCES2 (C) along with the RMSD plot of backbone atoms (D).

Table 6

Predicted activity, prime MMGBSA and glide score of best five mutual prodrugs from each linker category for hCES1 and hCES2.

Mutual prodrug ID	Structure	hCES1 (1YA8)			hCES2 (Homology model)		
Linker (Glycine)		Predicted hydrolytic activity ^a (pKm, μM)	ΔG MM-GBSA (kcal/mol) ^b	Glide score	Predicted hydrolytic activity ^c (pKm, μM)	ΔG MM-GBSA (kcal/mol) ^d	Glide score
EP-D1		4.474	-94.688	-5.891	4.202	-82.029	-6.947
EP-D4		5.221	-69.874	-7.566	4.104	-56.591	-4.375
EP-D12		4.229	-95.163	-4.542	4.051	-80.623	-5.105
EP-D19		4.422	-90.001	-6.649	4.185	-79.896	-5.579
EP-D24		4.795	-94.284	-8.432	4.134	-73.717	-5.790
Linker (β-alanine)		Predicted activity	MMGBSA	Glide score	Predicted activity	MMGBSA	Glide score
EP-E7		4.162	-81.818	-6.107	4.063	-65.461	-3.361
EP-E13		4.460	-59.464	-6.286	4.421	-75.363	-4.324
EP-E16		4.003	-100.804	-5.220	4.399	-76.764	-6.115
EP-E20		4.126	-115.006	-7.288	3.975	-79.108	-6.029
EP-E22		3.945	-81.882	-6.832	4.013	-43.715	-4.713
Linker (Phenylalanine)		Predicted activity	MMGBSA	Glide score	Predicted activity	MMGBSA	Glide score
EP-F3		4.642	-66.545	-6.616	4.246	-53.293	1.024
EP-F4		4.434	-56.411	-7.566	4.349	-68.518	-2.056
EP-F5		4.496	-64.073	-5.044	4.318	-63.931	-5.493

Table 6 (continued)

Mutual prodrug ID	Structure	hCES1 (1YA8)			hCES2 (Homology model)		
Linker (Glycine)		Predicted hydrolytic activity ^a (pKm, μM)	ΔG MM-GBSA (kcal/mol) ^b	Glide score	Predicted hydrolytic activity ^c (pKm, μM)	ΔG MM-GBSA (kcal/mol) ^d	Glide score
EP-F14		4.209	-85.549	-5.113	4.104	-73.394	-5.591
EP-F20		4.263	-80.540	-9.165	4.019	-82.934	-2.106
Mutual prodrugs without linker		Predicted activity (kcat/Km)	MMGBSA	Glide score	Predicted activity (kcat/Km)	MMGBSA	Glide score
EP-G1		3.833	-111.668	-7.665	4.393	-91.155	-5.111
EP-G3		4.190	-88.565	-4.958	4.592	-81.233	-5.471
EP-G7		3.952	-87.341	-7.337	3.423	-50.237	-6.580
EP-G12		4.420	-99.468	-4.953	3.952	-74.549	-6.758
EP-G15		4.187	-87.976	-6.362	3.984	-64.595	-5.792

Note: Km is the concentration of the substrate (prodrugs) at which half of the active site of the enzyme (hCES1 and hCES2) is filled and pKm is negative log of Km.

^a Activity predicted by AAHRR.430, PLS4.

^b Binding energy of prodrugs-hCES1 complex.

^c Activity predicted by AHHR.21, PLS2.

^d Binding energy of prodrugs -hCES2 complex.

the highest occupied molecular orbital (HOMO) of one reactant i.e. nucleophile to the lowest unoccupied molecular orbital (LUMO) of another reactant i.e. electrophile. The energy of HOMO (E_{HOMO}) parameterizes the electron donating ability of one reactant. Its higher value indicates more ability to donate electron than reactant with low HOMO. On the other hand, energy of LUMO (E_{LUMO}) parameterizes the electron accepting ability of the other reactant. Its low value indicates more ability to accept electron than reactant with a higher value of LUMO. For the comparative study of the hydrolytic cleavage of the designed prodrugs by nucleophilic substitution using hCES1 and hCES2 enzyme, the $E_{\text{Serine}} - E_{\text{Prodrugs}}$ gap, chemical hardness (η), electronic chemical potentials (μ) and the electrophilicity indices(u) of the reactants were considered as the most important parameters. These quantum-chemical descriptors were evaluated on the basis of the calculations of FMOs energies, i.e. HOMO and LUMO using the following equations (a-c) [45,46].

$$\mu = E_{\text{HOMO}} + E_{\text{LUMO}}/2 \quad (\text{equation a})$$

$$\eta = (E_{\text{LUMO}} - E_{\text{HOMO}})/2 \quad (\text{equation b})$$

$$\omega = \mu^2/2 \eta \quad (\text{equation c})$$

Since, the $E_{\text{Serine}} - E_{\text{Prodrugs}}$ energy gap was found to be large in case of EP-D9, EP-E9, EP-F9 and EP-G8 therefore, these prodrugs are not considered to be susceptible to get hydrolyzed by hCES1 and 2. Among all prodrugs, EP-F14 favored the hydrolysis by hCES1, as the HOMO-LUMO energy gap between both the prodrug and serine was less. On the other hand, EP-G15 is more susceptible to be hydrolyzed by hCES2 due to smaller energy gap. The value of μ for prodrugs EP-E13, EP-F14, EP-G12 and EP-F15 were found to be lower than that of μ of serine. This indicates the confirmed charge transfer between nucleophile (Serine) and electrophiles (prodrugs) in both cases. While the higher ω value for these prodrugs in comparison to serine revealed that these prodrugs are best electrophiles for being hydrolyzed by both hCES1 and 2. The aforementioned prodrugs satisfy all the required parameters for the hydrolysis i.e. angle, distance, energy gap and quantum chemical descriptors (μ , η , ω) values. The quantum chemical descriptors for all mutual prodrugs have been displayed in Table S3 (Supplementary data).

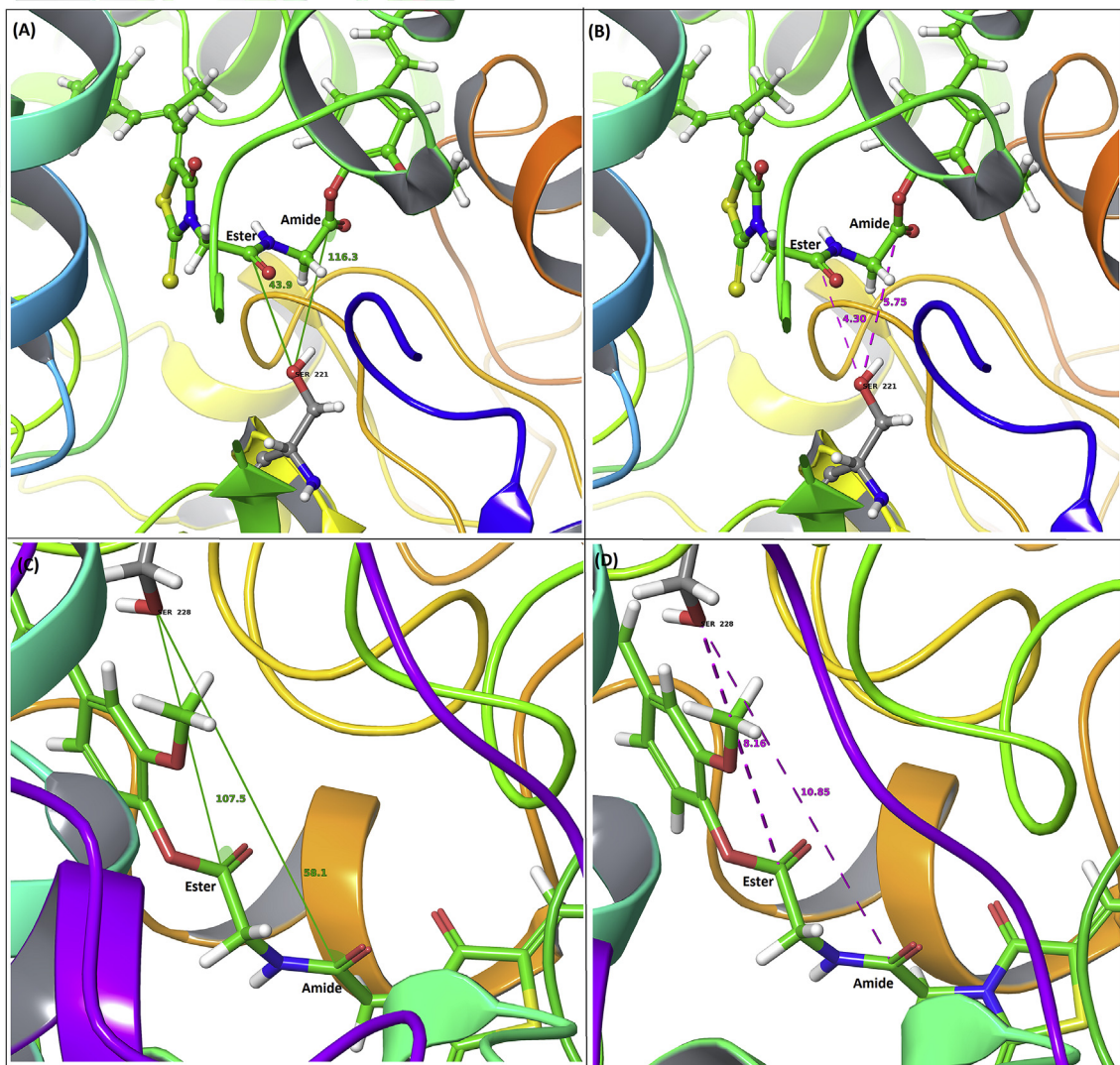


Fig. 10. Calculated Burgi-Dunitz angle between Ser221 and ester, amide carbonyl of EP-D19 (A), calculated distance between Ser221 and ester, amide carbonyl of EP-D19 (B), calculated Burgi-Dunitz angle between Ser228 and ester, amide carbonyl of EP-D19 (A), calculated distance between Ser228 and ester, amide carbonyl of EP-D19 (B).

3.8. Verloop's sterimol parameters

Verloop's sterimol approach was introduced in 1976 discussing different steric parameters which play an important role when any ligand interacts with a biological receptor. The six steric substituent parameters such as B1, B2, B3, B4, B5, and L were calculated for both components of mutual prodrugs i.e. Epalrestat (Acyl group) and Antioxidants (Alcoholic groups) which get hydrolyzed by esterase enzymes (hCES1 and hCES2). The catalytic domain of both hCES1 and 2 have different geometries with catalytic triad system i.e. Ser221, Glu354, His468 (hCES1) and Ser221, Glu354, His468 (hCES2). It is evident from the previous reports that both enzymes have the ability to accommodate different types of ligand. The hCES1 and hCES2 selectivity towards their substrate depend upon the size of their individual acyl and alkyl/aryl units. Published reports revealed that hCES 1 best accommodate ligand with small alkyl/aryl unit and large acyl unit, while hCES2 accommodates ligand containing large alkyl/aryl unit and small acyl unit due to its bigger catalytic domain [20]. To stand these reported results, sterimol descriptors were computed for individual acyl (Epalrestat) and alkyl/aryl (antioxidants) units. The computed Verloop's steric parameters include substituent length (L) and widths (B1, B2, B3, B4,

B5) [19]. The length of the substituent is measured in the direction in which it is attached to the parent molecule. The width of the alcohol and acyl unit is also as important as the length (L). Both the minimum width (B1) and maximum widths (B4, B5) are measured in a direction perpendicular to the length axis of the substituents [47]. Since the alcohol units (antioxidants) in the designed prodrugs were found to be smaller than the acyl unit (Epalrestat) in terms of their lengths (9.501–14.873 for alcohol units and 16.653 for acyl unit) and minimum width (1.661–2.855 for alcohol units and 2.867 for acyl unit), we concluded that the designed prodrugs are more susceptible to get cleaved by hCES1 than that of hCES2. However, the maximum width (B4, B5) is also crucial and have some correlation with the hydrolytic activity of hCES1 and hCES2. In some cases where the maximum width (B4, B5) of the alcoholic group is larger than that of an acyl group, there may be chances of these prodrugs to be hydrolyzed by hCES2 more efficiently than that of hCES1. Thus, we compared the maximum widths (B4, B5) of alcoholic groups in case of best (EP-D4) and worst (EP-G1) substrates of hCES1 and observed that alcoholic group of EP-D4 (6-Aminoflavone) manifested minimum B4 = 4.843 and B5 = 4.872 values whereas; alcoholic group of EP-G1 (3-Hydroxyflavone) possessed maximum value for B4 = 6.903 and B5 = 6.948. In the

Table 7

Geometrical parameters for the best five mutual prodrugs from each linker category.

Prodrug ID	hCES1				hCES2			
	Distance		Angle		Distance		Angle	
Glycine	Ester ^a	Amide ^a	Ester ^b	Amide ^b	Ester ^a	Amide ^a	Ester ^b	Amide ^b
EP-D1	8.37	8.79	113.8	37.2	8.54	11.54	123.9	80.4
	7.23	7.76	135.2	41.1	6.86	9.71	103.2	109.0
EP-D4	7.17	7.70	87.8	63.1	10.77	8.33	49.8	41.4
	4.73	5.50	109.6	65.2	9.07	6.35	61.5	48.4
EP-D12	8.25	7.37	126.2	13.8	9.30	11.25	111.3	69.5
	4.97	4.01	134.0	26.0	6.76	8.55	131.0	57.9
EP-D19	5.75	4.30	116.3	43.9	8.16	10.85	107.5	58.1
	5.00	3.89	99.9	85.2	7.49	10.11	88.7	60.1
EP-D24	8.14	8.02	160	44.4	10.68	13.83	96.1	103.2
	14.67	12.33	170.4	33.3	9.96	12.82	92.3	111.4
β-alanine								
EP-E7	5.85	9.36	46.7	115.2	15.36	17.85	91.9	135.0
	3.79	6.47	36.7	115.4	7.28	10.86	90.9	134.2
EP-E13	6.21	4.34	78.7	119.8	17.68	16.96	74.8	45.6
	5.40	5.29	111.5	72.6	13.58	12.49	78.1	43.2
EP-E16	6.19	9.97	33.4	72.2	8.49	11.88	30.0	68.9
	7.97	10.28	13.6	78.2	5.98	9.80	40.6	77.0
EP-E20	6.72	3.89	118.7	15.9	7.52	10.66	81.5	59.1
	5.73	8.18	145.4	91.4	5.00	8.39	32.7	59.7
EP-E22	4.83	5.88	57.6	42.1	12.70	13.87	97.6	45.1
	5.25	7.69	31.6	29.3	10.62	12.86	87.3	40.4
Phenylalanine								
EP-F3	5.22	8.00	63.3	92.2	10.59	14.07	43.0	117.6
	8.27	6.03	155.8	158.5	9.10	12.70	58.8	98.2
EP-F4	14.55	11.57	98.00	63.6	19.03	17.08	147.7	108.6
	11.04	7.90	107.7	70.3	19.98	17.69	135.3	96.5
EP-F5	5.85	3.34	110.6	100.9	13.82	15.94	72.7	97.5
	7.07	6.43	74.8	72.3	13.71	16.28	63.3	93.3
EP-F14	5.67	3.66	112.2	102.5	11.42	12.96	100.2	78.1
	6.27	3.80	100.3	20.7	11.33	13.46	86.7	88.9
EP-F20	8.43	6.33	60.1	46.6	18.80	15.73	120.6	76.6
	6.08	3.70	73.0	38.3	18.34	15.04	131.5	61.9
Ester linked								
EP-G1	8.50	—	67.3	—	14.96	—	66.6	—
	6.94		71.5		14.86		54.9	
EP-G3	6.17	—	30.5	—	10.93	—	58.3	—
	3.84		20.8		6.11		105.9	
EP-G7	10.17	—	96.8	—	4.39	—	77.2	—
	5.36		101.9		8.03		83.6	
EP-G12	3.71	—	68.1	—	11.64	—	116.1	—
	7.17		57.4		10.34		136.8	
EP-G15	6.55	—	83.0	—	11.32	—	114.3	—
	3.69		72.3		8.76		109.6	

^a The first value indicates the distance between carbonyl carbon of either ester or amide and oxygen of serine, while the second value indicates the distance between carbonyl carbon of either ester or amide and catalytic water.

^b The first value indicates the angle between carbonyl carbon, carbonyl oxygen of either ester or amide and oxygen of serine, while the second value indicates the angle between carbonyl carbon of either ester or amide and oxygen of catalytic water.

light of the above, it can be concluded that B4 and B5 values must be lower for better hydrolytic activity of hCES1, vice versa in case of hCES2. EP-D19, a good substrate for both the enzymes, was found to have a maximum width (B4, B5 = 6.05) which lies in between the B4 and B5 values of EP-D4 (4.843, 4.872) and EP-G1 (6.903, 6.948). The steric parameters for all substituents used during the study have been mentioned in Table 8.

4. Concluding remarks and future perspectives

Recurrent failure in the management of DC signals the need for novel therapeutic interventions. Epalrestat, the only drug currently available against diabetic complications is prescribed as immediate release drug and can only target the upstream pathway (polyol pathway) thus; there are chances for the disease to progress through some other pathways like downstream pathway (oxidative stress). Oxidative stress is the triggering factor for all the remaining pathways of DC. Under this scenario, transforming the epalrestat

into other agents, in the form of antioxidants linked mutual prodrugs, with and without linkers, can be a fascinating approach to target both upstream and downstream pathways of DC owing to a synergistic effect with sustained release property and improved elimination half-life. Further understanding of the biotransformation of these prodrugs is necessary for their effective designing. Since hCES1 & hCES2 are the main contributory enzymes in prodrug activation which hydrolyze the ester and amide containing prodrugs, their study at the molecular level is highly desirable. Thus, our study aimed to solve the enigma of the hydrolytic mechanism at the molecular level using *in-silico* techniques which helped in designing of mutual prodrugs in very cost-effective manner. To achieve this, initially, ligand-based pharmacophore models were generated and validated for both hCES1 and 2 to find out the essential features required to get hydrolyzed by these enzymes. Further docking study was performed to dig out essential interactions with key amino acids (ser221, ser228) followed by molecular dynamics simulations to assure the stability of the complex.

Table 8

Verloop's sterimol parameters.

Type of group	Name of promoiety	B1	B2	B3	B4	B5	L
Acyl group	Epalrestat	2.867	3.719	3.809	4.757	5.002	16.653
Alcohol group	3-Hydroxyflavone	1.835	1.873	2.962	6.903	6.948	14.042
Alcohol group	4-Hydroxycoumarin	1.661	2.364	2.398	6.329	6.329	9.727
Alcohol group	5-Hydroxyflavone	2.157	2.471	2.758	6.007	6.024	14.184
Alcohol group	6-Aminoflavone	2.127	2.423	3.901	4.843	4.872	14.831
Alcohol group	6-Hydroxyflavone	2.206	2.314	3.821	4.935	4.955	14.717
Alcohol group	6-Hydroxyflavanone	2.855	3.22	3.86	4.763	4.806	14.651
Alcohol group	7-Hydroxyflavone	1.836	1.986	2.555	7.134	7.166	14.144
Alcohol group	Butylated hydroxyl anisole	2.627	3.617	3.657	6.544	6.545	10.859
Alcohol group	BQ-2-Chlorocatechol	2.816	3.286	3.381	4.376	4.576	12.809
Alcohol group	BQ-2-Cl-Phenol	2.531	3.094	3.767	4.501	4.645	12.587
Alcohol group	BQ-2-Naphthol	2.855	2.925	3.976	4.259	4.322	14.873
Alcohol group	BQ-2-Nitrophenol	2.295	3.243	3.619	5.036	5.04	12.488
Alcohol group	BQ-O-cresol	2.504	3.153	3.173	5.059	5.129	12.527
Alcohol group	BQ-phenol	2.509	2.638	3.493	4.056	4.144	12.694
Alcohol group	Chrysin	2.837	2.894	5.176	6.038	6.039	12.753
Alcohol group	Eugenol	2.536	2.68	3.343	6.033	6.048	11.528
Alcohol group	Guaiacol	1.721	2.275	2.297	6.492	6.492	9.924
Alcohol group	Lawson	2.336	2.43	2.911	5.717	5.717	10.05
Alcohol group	Methyl-Ferulic acid	2.274	2.28	2.767	6.05	6.05	14.18
Alcohol group	Menthol	1.721	2.474	4.17	6.079	6.241	11.286
Alcohol group	Sesamol	2.187	2.198	2.972	4.818	4.818	9.501
Alcohol group	Thymol	1.721	3.327	3.781	6.169	6.192	10.901
Alcohol group	Umbelliferone	1.909	1.913	3.164	4.732	4.732	10.495
Alcohol group	Vanillin	1.721	2.256	2.317	6.88	6.88	10.52

Quantum mechanical, geometrical and sterimol descriptors further validated the substrate capabilities of the designed prodrugs. On the basis of *in-silico* study, we sought that prodrug EP-D19 is the best substrate for both the enzymes while prodrug EP-F5 best fit into the catalytic domain of hCES1 than that of hCES2. Results of Verloop's sterimol approach suggested that designed prodrugs are better substrates for hCES1 than that of hCES2. For a prodrug to be a better substrate for hCES1, the size of acyl group should be larger than its alcoholic counterpart. However, the wide binding pocket of hCES1 sometimes allows it to act on structurally distinct compounds of either large or small alcohol moiety. On the other hand, hCES2 recognizes a substrate with a large alcohol group and small acyl group and its substrate specificity is limited. The specificity of hCES2 for the substrates may be restricted due to conformational interference in the binding pocket as a result of acyl-hCES2 conjugate formation. Since the acyl group in almost all reported prodrugs are larger than their alcohol part, it can be the primary reason for all designed prodrugs to be more susceptible to get hydrolyzed by hCES1 than hCES2. Moreover, hCES1 is responsible for high transesterification activity which may be another reason for high substrate specificity.

Disclosure statement

No potential conflict of interest was declared by the authors.

Acknowledgment

Author(s) would like to thank the Indian Council of Medical Research, New Delhi for providing financial assistance in the form of a fellowship during this work and express sincere gratitude towards Ms. Himanshu Verma, DPSR, Punjabi University, Patiala for her help and support throughout the study.

Appendix A. Supplementary data

Supplementary data to this article can be found online at <https://doi.org/10.1016/j.jmgm.2019.06.012>.

Funding

This work was supported by the Indian Council of Medical Research (ICMR) New Delhi under grant no. ISRM/11(61)/2017.

References

- [1] N. Hotta, R. Kawamori, M. Fukuda, Y. Shigeta, Group, A.R.I.D.C.T.S., Long-term clinical effects of epalrestat, an aldose reductase inhibitor, on progression of diabetic neuropathy and other microvascular complications: multivariate epidemiological analysis based on patient background factors and severity of diabetic neuropathy, *Diabet. Med.* 29 (2012) 1529–1533.
- [2] J.W. Steele, D. Faulds, K.L. Goa, Epalrestat, *Drugs Aging* 3 (1993) 532–555.
- [3] X. Li, Y. Shen, Y. Lu, J. Yang, Amelioration of bleomycin-induced pulmonary fibrosis of rats by an aldose reductase inhibitor, epalrestat, *Korean J. Physiol. Pharmacol.* 19 (2015) 401–411.
- [4] M.A. Ramirez, N.L. Epalrestat Borja, An aldose reductase inhibitor for the treatment of diabetic neuropathy, *Pharmacotherapy: J. Human Pharmacol. Drug Ther.* 28 (2008) 646–655.
- [5] M. Brownlee, Biochemistry and molecular cell biology of diabetic complications, *Nature* 414 (2001) 813.
- [6] H.F. Root, W.H. Pote, H. Frehner, Triopathy of diabetes: sequence of neuropathy, retinopathy, and nephropathy in one hundred fifty-five patients, *AMA Arch. Intern. Med.* 94 (1954) 931–941.
- [7] N. Hotta, N. Sakamoto, Y. Shigeta, R. Kikkawa, Y. Goto, Clinical investigation of epalrestat, an aldose reductase inhibitor, on diabetic neuropathy in Japan: multicenter study, *J. Diabetes Complicat.* 10 (1996) 168–172.
- [8] Y. Goto, N. Hotta, Y. Shigeta, N. Sakamoto, R. Kikkawa, Effects of an aldose reductase inhibitor, epalrestat, on diabetic neuropathy. Clinical benefit and indication for the drug assessed from the results of a placebo-controlled double-blind study, *Biomed. Pharmacother.* 49 (1995) 269–277.
- [9] N. Hotta, N. Sakamoto, Y. Shigeta, R. Kikkawa, Y. Goto, Clinical investigation of epalrestat, an aldose reductase inhibitor, on diabetic neuropathy in Japan: multicenter study, in: D.N.S.G. Japan (Ed.), *J. Diabetes Complicat.* 10 (1996) 168–172.
- [10] I. Kalofonos, J. Caron, W. Martin-Doyle, Modified Release Compositions of Epalrestat or a Derivative Thereof and Methods for Using the Same, Google Patents, 2018.
- [11] A. Ceriello, New insights on oxidative stress and diabetic complications may lead to a “causal” antioxidant therapy, *Diabetes Care* 26 (2003) 1589–1596.
- [12] F. Giacco, M. Brownlee, Oxidative stress and diabetic complications, *Circ. Res.* 107 (2010) 1058–1070.
- [13] A. Maritim, a. Sanders, J. Diabetes Watkins Iii, Oxidative stress, and antioxidants: a review, *J. Biochem. Mol. Toxicol.* 17 (2003) 24–38.
- [14] O. Phuangswai, S. Hannongbua, M.P. Gleeson, Elucidating the origin of the esterase activity of human serum albumin using QM/MM calculations, *J. Phys. Chem. B* 118 (2014) 11886–11894.
- [15] R. Karaman, B. Fattash, A. Qtait, The future of prodrugs—design by quantum

- mechanics methods, *Expert Opin. Drug Deliv.* 10 (2013) 713–729.
- [16] W. Hakamata, S. Tamura, T. Hirano, T. Nishio, Multicolor imaging of endoplasmic reticulum-located esterase as a prodrug activation enzyme, *ACS Med. Chem. Lett.* 5 (2014) 321–325.
- [17] M.K. Danks, C.L. Morton, E.J. Krull, P.J. Cheshire, L.B. Richmond, C.W. Naeve, et al., Comparison of activation of CPT-11 by rabbit and human carboxylesterases for use in enzyme/prodrug therapy, *Clin. Cancer Res.* 5 (1999) 917–924.
- [18] T. Satoh, M. Hosokawa, The mammalian carboxylesterases: from molecules to functions, *Annu. Rev. Pharmacol. Toxicol.* 38 (1998) 257–288.
- [19] A. Verloop, W. Hoogenstraaten, J. Tipker, Development and Application of New Steric Substituent Parameters in Drug Design. in: *Drug Design*, vol. 7, Elsevier, 1976, pp. 165–207.
- [20] B. Vyas, S. Choudhary, P.K. Singh, A. Singh, M. Singh, H. Verma, et al., Molecular dynamics/quantum mechanics guided designing of natural products based prodrugs of Epalrestat, *J. Mol. Struct.* 1171 (2018) 556–563.
- [21] A. Kaur, B. Singh, B. Vyas, O. Silakari, Synthesis and biological activity of 4-aryl-3-benzoyl-5-phenylspiro [pyrrolidine-2,3'-indolin]-2'-one derivatives as novel potent inhibitors of advanced glycation end product, *Eur. J. Med. Chem.* 79 (2014) 282–289.
- [22] T. Satoh, P. Taylor, W.F. Bosron, S.P. Sanghani, M. Hosokawa, B.N. La Du, Current Progress on Esterases: from Molecular Structure to Function, *ASPET*, 2002.
- [23] G. Vistoli, A. Pedretti, A. Mazzolari, B. Testa, In silico prediction of human carboxylesterase-1 (hCES1) metabolism combining docking analyses and MD simulations, *Bioorg. Med. Chem.* 18 (2010) 320–329.
- [24] S.L. Dixon, A.M. Smolyrev, E.H. Knoll, S.N. Rao, D.E. Shaw, R.A. Friesner, PHASE: a new engine for pharmacophore perception, 3D QSAR model development, and 3D database screening: 1. Methodology and preliminary results, *J. Comput. Aided Mol. Des.* 20 (2006) 647–671.
- [25] M. Kaur, O. Silakari, Ligand-based and e-pharmacophore modeling, 3D-QSAR and hierarchical virtual screening to identify dual inhibitors of spleen tyrosine kinase (Syk) and janus kinase 3 (JAK3), *J. Biomol. Struct. Dyn.* 35 (2017) 3043–3060.
- [26] B. Vyas, M. Singh, M. Kaur, O. Silakari, M.S. Bahia, B. Singh, Pharmacophore and docking-based hierarchical virtual screening for the designing of aldose reductase inhibitors: synthesis and biological evaluation, *Med. Chem. Res.* 25 (2016) 609–626.
- [27] M. Kaur, A. Kumari, M.S. Bahia, O. Silakari, Designing of new multi-targeted inhibitors of spleen tyrosine kinase (Syk) and zeta-associated protein of 70 kDa (ZAP-70) using hierarchical virtual screening protocol, *J. Mol. Graph. Model.* 39 (2013) 165–175.
- [28] B. Webb, A. Sali, Protein structure modeling with MODELLER, in: *Functional Genomics*, Springer, 2017, pp. 39–54.
- [29] S.F. Altschul, W. Gish, W. Miller, E.W. Myers, D.J. Lipman, Basic local alignment search tool, *J. Mol. Biol.* 215 (1990) 403–410.
- [30] M.J. Sippl, Recognition of errors in three-dimensional structures of proteins, *Proteins: Struct. Func. Bioinform.* 17 (1993) 355–362.
- [31] M. Wiederstein, M.J. Sippl, ProSA-web: interactive web service for the recognition of errors in three-dimensional structures of proteins, *Nucleic Acids Res.* 35 (2007) W407–W410.
- [32] P. Benkert, S.C. Tosatto, D. Schomburg, QMEAN: A comprehensive scoring function for model quality assessment, *Proteins: Struct. Func. Bioinform.* 71 (2008) 261–277.
- [33] S. Agnihotri, R. Narula, K. Joshi, S. Rana, M. Singh, In silico modeling of ligand molecule for non structural 3 (NS3) protein target of flaviviruses, *Bio-information* 8 (2012) 123.
- [34] M. Kaur, M.S. Bahia, O. Silakari, Exploring the role of water molecules for docking and receptor guided 3D-QSAR analysis of naphthyridine derivatives as spleen tyrosine kinase (Syk) inhibitors, *J. Chem. Inf. Model.* 52 (2012) 2619–2630.
- [35] C.D. Fleming, S. Bencharit, C.C. Edwards, J.L. Hyatt, L. Tsurkan, F. Bai, et al., Structural insights into drug processing by human carboxylesterase 1: tamoxifen, mevastatin, and inhibition by benzil, *J. Mol. Biol.* 352 (2005) 165–177.
- [36] P.K. Singh, O. Silakari, Molecular dynamics guided development of indole based dual inhibitors of EGFR (T790M) and c-MET, *Bioorg. Chem.* 79 (2018) 163–170.
- [37] M. Kaur, M. Singh, O. Silakari, Oxindole-based SYK and JAK3 dual inhibitors for rheumatoid arthritis: designing, synthesis and biological evaluation, *Future Med. Chem.* 9 (2017) 1193–1211.
- [38] D. Pathak, N. Chadha, O. Silakari, Identification of non-resistant ROS-1 inhibitors using structure based pharmacophore analysis, *J. Mol. Graph. Model.* 70 (2016) 85–93.
- [39] J. Foresman, E. Frish, *Exploring Chemistry*, Gaussian Inc., Pittsburg, USA, 1996.
- [40] A. Varandas, J. Brandao, A simple semi-empirical approach to the intermolecular potential of van der Waals systems: I. Isotropic interactions: application to the lowest triplet state of the alkali dimers, *Mol. Phys.* 45 (1982) 857–875.
- [41] K.N. Houk, Frontier molecular orbital theory of cycloaddition reactions, *Acc. Chem. Res.* 8 (1975) 361–369.
- [42] P. Chattaraj, A. Poddar, Molecular reactivity in the ground and excited electronic states through density-dependent local and global reactivity parameters, *J. Phys. Chem. A* 103 (1999) 8691–8699.
- [43] E. Pontiki, D. Hadjipavlou-Litina, QSAR models on H4 receptor antagonists associated with inflammation and anaphylaxis, *J. Biomol. Struct. Dyn.* 35 (2017) 968–1005.
- [44] C.A. Lipinski, Lead-and drug-like compounds: the rule-of-five revolution, *Drug Discov. Today Technol.* 1 (2004) 337–341.
- [45] M. Karelson, V.S. Lobanov, A.R. Katritzky, Quantum-chemical descriptors in QSAR/QSPR studies, *Chem. Rev.* 96 (1996) 1027–1044.
- [46] P. Thanikaivelan, V. Subramanian, J.R. Rao, B.U. Nair, Application of quantum chemical descriptor in quantitative structure activity and structure property relationship, *Chem. Phys. Lett.* 323 (2000) 59–70.
- [47] A. Verloop, J. Tipker, A comparative study of new steric parameters in drug design, *Pharmacochem. Libr.* 2 (1977) 63–81.